Scanning Microscopy

Volume 3 | Number 1 Article 8

3-1-1989

# Prospects for Photo Electron Spectroscopy in a Scanning Transmission Electron Microscope

F. J. Pijper
*Delft University of Technology*

A. J. Bleeker
*Delft University of Technology*

R. J. Endert
*Delft University of Technology*

P. Kruit
*Delft University of Technology*

Scanning Microscopy, Vol. 3, No. 1, 1989 (Pages 65-69) 0891-7035/89$3.00+.00
Scanning Microscopy International, Chicago (AMF O'Hare), IL 60666 USA

# PROSPECTS FOR PHOTO ELECTRON SPECTROSCOPY IN A SCANNING TRANSMISSION ELECTRON MICROSCOPE

F.J. Pijper*, A.J. Bleeker, R.J. Endert and P. Kruit.

Department of Applied Physics,
Delft University of Technology,
Lorentzweg 1, 2628 CJ Delft, The Netherlands.

(Received for publication January 16, 1989, and in revised form March 1, 1989)

## Abstract

High spatial resolution microanalysis in scanning transmission electron microscopes is most easily performed when the specimen is inside a magnetic immersion objective lens. Recently a technique has been developed to perform spectroscopy of electrons that originate in this magnetic field. A very special form of photo electron spectroscopy is then possible for thin specimens in the microscope. An energy loss $\Delta E$ of a primary electron has the same physical effect as the absorption of a photon of energy $\Delta E$. A coincidence measurement between energy loss electrons and the emitted electrons is expected to give a so called coincidence electron spectrum, or (e,2e) spectrum, of a very small area, which gives the same physical information as photo electron spectroscopy. Normal photo electron spectroscopy of limited spatial resolution, but with high collection efficiency, should also be possible in a scanning transmission electron microscope if the specimen is illuminated with a photon beam. Experiments to test the expectations are in progress.

KEYWORDS : Surface Microanalysis, Scanning transmission electron microscopy, Spatial Resolution, Photo electron spectroscopy, Ejected electron spectroscopy, Coincidence electron spectroscopy.

* Address for correspondence:
F.J. Pijper
Research Group Particle Optics
Lorentzweg 1
2628 CJ Delft, The Netherlands
Phone No 31-15-786077

## Introduction

For elemental analysis in scanning transmission electron microscopy (STEM), techniques such as diffraction, electron energy loss spectroscopy (EELS) and energy dispersive X-ray analysis (EDX) are readily available. The highest spatial resolution is always obtained using magnetic immersion objective lenses. Recently the possibility of Auger electron spectroscopy (AES) in STEM has been demonstrated (Kruit (1986), Kruit and Venables (1988)). This involves the spectroscopy of electrons originating in the magnetic field of the objective lens. When spectroscopy of relatively low energy electrons is possible in STEM, the logical next question is: can we do photo electron spectroscopy in the same instrument, preferably also with high spatial resolution? In this paper we discuss three possibilities for photo electron spectroscopy in STEM and describe the state of development of experiments along these lines in Delft. Improvements in the spatial resolution of electron spectroscopy for chemical analysis (ESCA) with instruments other than STEMs, have been reviewed recently by Cazaux (1984a,1985) and Chaney (1987), and will therefore not be discussed in this paper.

## Electron Spectroscopy in STEM

In Delft we have modified a Philips EM400 transmission electron microscope to test the possibility of new electron spectroscopy techniques (fig. 1). The upper part of the objective lens has been changed and now includes an extra coil, which prevents the magnetic field from dropping to zero in the rest of the objective lens. A gradually decreasing field is obtained, which abruptly stops at the position of a magnetic aperture, located between the condenser lenses and the objective lens. Electrons originating in a specimen which is located in the high field region, will start spiraling with a cyclotron orbit of small radius. In the decreasing field the electrons will follow orbits of larger radius (inversely proportional to the square root of the field), meanwhile being parallelized, by which we mean that the transverse velocity is converted almost completely into forward velocity. The electrons that pass the magnetic aperture are separated from the primary beam in an electrostatic $90^\circ$ hemispherical deflector and are focused on the entrance slit of a $180^\circ$ concentric hemispherical analyzer (CHA). The first experimental spectra show an energy resolution (FWHM) below 1 eV for Auger electrons of 200 to 1400 eV (Ar LMM and Al KLL peaks).

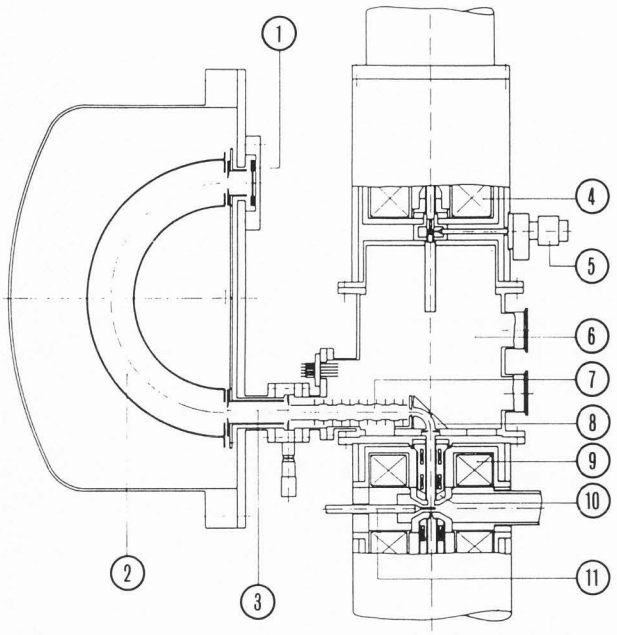


Fig. 1. Experimental set-up for testing the electron spectroscopy techniques. 1) electron detector, 2) CHA, 3) beam defining slits, 4) second condenser lens, 5) condenser diaphragm, 6) microscope extension, 7) electrostatic lenses, 8) 90° deflector, 9) objective lens, 10) parallelizing coils, 11) specimen rod.

## Coincidence Electron Spectroscopy

In the past, alternatives for expensive, high intensity photon sources, necessary for photo electron spectroscopy, have been looked for and were found in coincidence electron spectroscopy. Coincidence electron spectroscopy is also called (e,2e) spectroscopy, because processes are examined where one electron goes in and two electrons come out. If the energy loss involved is small compared to the energy of the incoming electron the term near dipole (e,2e) is used, to distinguish it from low energy (e,2e), where large scattering angles are involved. Near dipole (e,2e) experiments on gases, of course without spatial resolution, have been reported among others by Van der Wiel and Brion (1972/73), Haak et al. (1984) and Ungier and Thomas (1985).

In normal photo electron spectroscopy (XPS and UPS) incident photons are absorbed by the specimen under study. In the process of photo ionization of an atom an electron is ejected. The kinetic energy $E_k$ of the photo electron equals the photon energy $h\nu$ minus the ionization energy $E_B$. Electrons from the primary beam in an electron microscope also cause ionization of sample atoms. According to Jackson (1962) the similarity between these processes is found in the method of virtual quanta. During the interaction time the electron offers the atom a white photon spectrum from which it can choose any ionization energy. The energy of the virtual photon, absorbed by the sample atom, is unfortunately not known beforehand, as it is when a photon from a monochromatic source is being absorbed. In thin samples however, detection of the energy loss electron provides this information. The kinetic energy of the ejected electron, will be the selected energy loss $\Delta E$ minus the ionization energy $E_B$, independent of the energy of the incident primary electron (fig. 2).

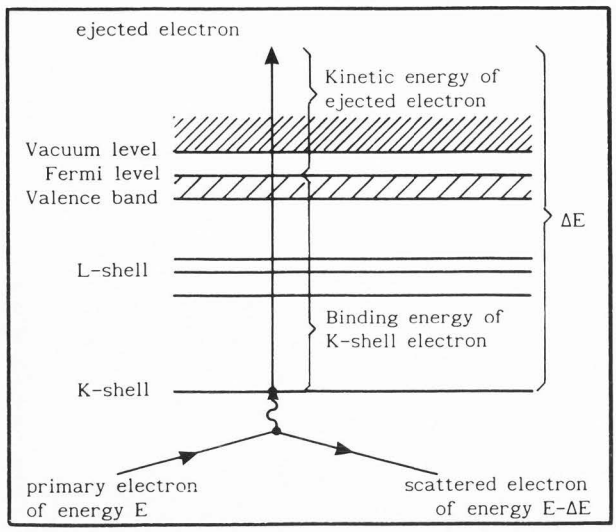


Fig. 2. Schematic energy level diagram with basic atomic mechanism involved in coincidence electron spectroscopy.

The ejection of the electron will take place almost immediately after passage of the primary electron. Therefore there is a close time relation between the arrival of the transmitted and ejected electrons at their respective detectors.

Coincidence techniques can be used to select only those electrons that arrive within a time window $\tau$ around this time difference. The smaller $\tau$ can be chosen, the smaller the background due to false coincidences will be. Assuming that the rate of true coincidences is small compared to both the total signal in the EELS detector $R_E$ and the total signal in the secondary electron detector $R_S$, the rate of false coincidences $R_F$ depends linearly on $R_E$, $R_S$ and $\tau$. The background in the coincidence spectrum will have the same form as the non-coincident electron spectrum and can in principle be subtracted. In our experiment $\tau$ is expected to be in the order of 10 nanoseconds, mainly due to different flight paths inside the secondary electron analyzer.

The coincidence electron count rate per illuminated atom in the surface layer is given by:

$$R_a = \frac{J_0}{e} \cdot \sigma \cdot T_E \cdot \varepsilon \cdot T_P \qquad (1)$$

where $J_0$ is the electron density in the primary electron beam. $J_0$ can be as high as 1 nA/nm$^2$ with a field emission source and an acceleration voltage of 100 kV. When expressed in electron counts this is about $6 \cdot 10^9$ el/s in a 1 nm$^2$ spot. $\sigma$ is the probability of ionization for the selected energy loss band, that is the partial ionization cross section. The partial cross section for carbon, for an accepted energy band of 1 eV, about 30 eV above the K-edge is found to be about $1.3 \cdot 10^{-22}$ cm$^2$ (using the program SIGMAK2 described by Egerton (1986)). The width of the band also determines the energy resolution in the coincidence electron spectrum, so this restricts the cross section. In principle, it is possible to use a multiple detector for the energy loss measurements and thus effectively illuminate the sample with different wavelength photons at the same time. This is however complicated in a coincidence measurement. We use carbon K-shell ionization as an example here, but are aware that heavier elements have partial cross sections for the K-shell down to two orders of magnitude smaller. On the

other hand L-shell and valence band ionization cross sections can be two orders of magnitude larger. $T_E$ is the collection efficiency for energy loss electrons. Inelastic scattering is primarily in forward direction. Objective lens and spectrometer aberrations limit the range of scattering angles that can be accepted, see Kruit and Shuman (1985). In our set-up we find a 50 mrad acceptance angle, for an energy resolution of 1 eV. With an expected quantum detection efficiency of 80 % for the EELS detector (plastic scintillator and photomultiplier), this leads to a $T_E$ of 0.8. $\varepsilon$ is the fraction of the electrons which have a velocity component towards the secondary electron analyzer and is a function of the exact angular distribution of the ejected electrons. This distribution is equivalent to that of electrons ejected by unpolarized light propagating parallel to the microscope axis, see Kim (1972). An asymmetry parameter $\beta$, which is transition dependent, determines the form of the distribution. The distribution is symmetrical around the plane perpendicular to the incoming beam, which means that half of the electrons is traveling backward, giving $\varepsilon = 0.5$. $T_P$ is the collection efficiency for photo electrons. The collection efficiency of a parallelizer with a CHA is discussed by Kruit and Venables (1988) and is expected to be close to 1 for electrons up to 300 eV and remains above 60 % for electrons up to 1000 eV energy, with a resolution better than 1 eV. As for the EELS detector, the quantum detection efficiency of the secondary electron detector (a chevron microchannel plate) can be as high as 80 % , so that for the ejected electrons of 30 eV energy the collection efficiency $T_P$ is 0.8.

These numbers lead to an expected count rate of 26 coincidence electrons per sec per atom, if we have a spot of 1 $nm^2$, for the K-shell ionization of carbon. To find the total count rate of coincidence electrons from a surface layer, we have to multiply this amount by the number of atoms in the volume contributing to the coincidence electron spectrum, which is a factor $\lambda_{esc} \cdot A \cdot N_A$. $\lambda_{esc}$ is the escape depth of the electrons, which is similar to the escape depth known in photo electron spectroscopy. Unfortunately data for $\lambda_{esc}$ are scarce for energies around 30 eV, see Seah and Dench (1979) and Tanuma et al. (1988). For $\lambda_{esc}$ in carbon we will use an estimate of 0.35 nm, (Seah and Dench (1979), especially formulas 1 and 12). A is the area 'illuminated' by the primary electron beam (1 $nm^2$) and $N_A$ is the atomic density of the species under study (100 $nm^{-3}$ for pure carbon). With these values we can expect a true coincidence count rate $R_T$ of 900 electrons per second.

We will make an estimate of the false coincidence count rate for an imaginary situation of a single carbon atom (index 1) on top of an aluminum background (index 2) of thickness t.

An estimate of the EELS signal is given by the contribution of the background material:

$$R_E = \frac{J_0}{e} \cdot \sigma_2 \cdot N_{A,2} \cdot A \cdot t \cdot T_E \qquad (2)$$

If we assume that $\sigma_2$ is dominated by the Al L-edge and not by plasmon losses, we find a cross section of $1.9 \cdot 10^{-22}$ $cm^2$, at 315 eV loss, (30 eV above the carbon edge), using the program SIGMAL2, described by Egerton (1986). The background in the secondary electron spectrum can be estimated if we combine the knowledge about the secondary electron yield $\delta$ and the shape of the secondary electron spectrum g(E). According to Chung and Everhart (1974) the shape mainly depends on the workfunction $W_f$ of the material and can be expressed as:

$$g(E) = \frac{E}{(E+W_f)^4} \qquad (3)$$

The integral over g(E) from zero to infinity must be equal to $\delta$. An estimate for the background in the secondary electron spectrum is then :

$$R_S = 6 \cdot W_{f,2}^2 \cdot \delta_2 \cdot \int_{30}^{31} \frac{E}{(E+W_{f,2})^4}\, dE \cdot \frac{J_0}{e} \cdot A \cdot T_P \qquad (4)$$

The resulting ratio of true over false coincidences for a single atom on top of the background is now:

$$\frac{R_a}{R_F} = \frac{\sigma_1 \cdot \varepsilon}{6 \cdot W_{f,2}^2 \cdot \delta_2 \cdot \int_{30}^{31} \frac{E}{(E+W_{f,2})^4}\, dE \cdot \sigma_2 \cdot N_{A,2} \cdot \frac{J_0}{e} \cdot A^2 \cdot t \cdot \tau} \qquad (5)$$

With a secondary electron yield of 2 % for aluminum at 100 keV (see Reimer (1983)), a workfunction of 4 eV, an atomic density in aluminum of 60 $nm^{-3}$, a thickness of 10 nm and the rest as given above, this yields a ratio of 0.2. If, instead of just considering a single atom, small clusters of carbon atoms are examined, this ratio is increased with the number of atoms in the cluster. For larger clusters the escape depth in the surface layer will limit the ratio of true over false coincidences. Of course this is only an example and the ratio is strongly dependent on the choice of parameters and materials. From the last formula one can also see that both a smaller time window $\tau$ and a smaller primary beam current $I_0$ (= $J_0 \cdot A$) improves the signal to background ratio (as in any coincidence technique). The signal to noise ratio (Poisson distributed noise on signal plus background) will however be constant or even decrease with smaller current.

We have built the experimental set-up in the non-UHV system described in fig. 1 and expect to obtain coincidence spectra very soon, although the development of this technique for practical analysis of uncontaminated surfaces will require a fully UHV instrument. We presently have one under construction in Delft.

## Selected Area Photo Electron Spectroscopy

Even without localized electron production a magnetic parallelizer can be used to give some spatial resolution. Beamson et al. (1980) have used the magnifying properties of the magnetic parallelizer to obtain magnified photo electron images, see also Turner et al. (1984)

In our set-up a magnified image of the central region of the specimen is formed at the position of the magnetic aperture (fig. 3). The aperture selects the central area of the image. When the aperture plane is imaged on the entrance slit of the CHA, energy analysis can be done on the electrons that contribute to this area. The spatial resolution obtainable will be in the order of the cyclotron diameter of the electrons in the magnetic field at the specimen plane (Kruit and Read, 1983).

For a magnetic field of 1 Tesla, the spatial resolution of for example 250 eV electrons will be about 100 $\mu$m. Of course this cannot be regarded as high spatial resolution, but it provides the possibility to compare coincidence electron spectroscopy with normal photo electron spectroscopy in the same instrument.

Incident X-rays can be produced either inside or outside the microscope by illumination of a target with high energy electrons. The photon density $J_{ph}$ is linearly proportional to the primary electron current $I_0$ and inversely proportional to the square root of the distance L between the X-ray source and the specimen. Commercial

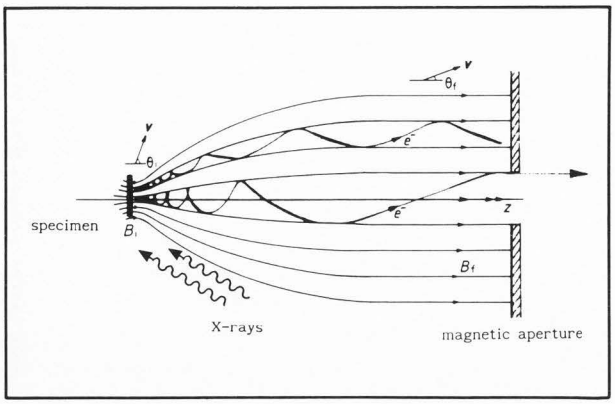


Fig. 3. Principle of selected area technique.

water cooled X-ray sources operate with electron currents in the order of 10 mA, but cannot be mounted closer to the specimen than about 10 cm (in our instrument).

We are developing a method in which the primary beam of the microscope, operated with a current of 1 $\mu$A, hits an uncooled aluminum target at 1 mm distance from the object under study. Because the target is also in the high magnetic field, this is far enough to prevent secondary electrons originating in the target from reaching the detector. It should yield the same photon flux on the object as a large X-ray source would yield, when mounted on the outside of the microscope.

## Microprobe Photo Electron Spectroscopy

The idea of using microprobe X-rays to do photo electron spectroscopy has been extensively reported by Cazaux (1984a,b). An electron beam, when focused on an anode foil can create localized X-rays on a specimen which is attached to the back of the anode (fig. 4). The

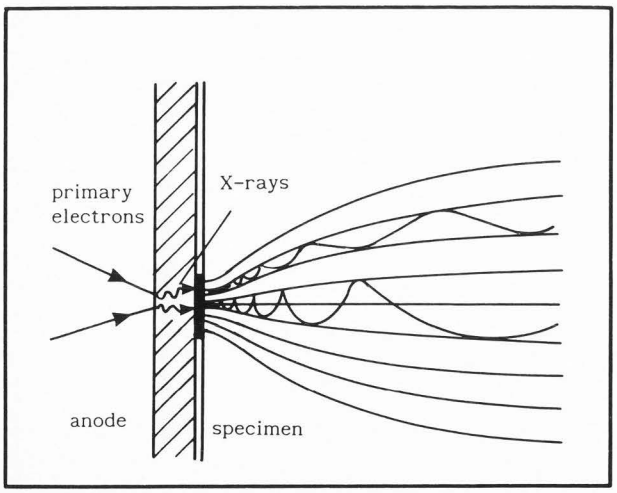


Fig. 4. Principle of microprobe technique.

resolution is limited to the size of the transmitted X-ray spot (0.5-10 $\mu$m). Of course this method could also be employed in STEM, in combination with a magnetic parallelizer for high collection efficiency. If the standard electron gun is being used to create X-rays, a parallelizer and analyzer need to be built on the other side of the objective lens, as has been done by Venables, see Kruit and Venables (1988). Alternatively an additional electron gun, pointing upwards (for example, somewhere inside the viewing chamber) might be used.

## Conclusions

In this paper three possibilities for photo electron spectroscopy in a STEM have been discussed. Especially the coincidence electron spectroscopy technique is expected to have very exciting capabilities. Not only the flexibility of choice of photon energy, as in synchrotron radiation, but also the spatial resolution of the order of STEM probes (1 nm$^2$) have not been reported before. The selected area photo electron spectroscopy method, with X-rays produced at a close distance to the sample using the primary electron beam, has good capabilities to compare the coincidence electron spectroscopy with normal photo electron spectroscopy. It lacks however the very high spatial resolution. The microprobe photo electron spectroscopy method can be incorporated in STEM as well, and gain in collection efficiency is expected in combination with a magnetic parallelizer. The main disadvantage of this technique is the need to attach the specimen to an anode foil, which makes it impossible to do transmission electron microscopy in the same set-up.

The practical usefulness of these techniques awaits further experimental evidence, but preliminary results are promising.

## Acknowledgement

This project is supported by the Dutch Technology Foundation (STW Project DTN-44.0745) and by Philips BV.

## References

Beamson G, Porter HQ, Turner DW (1980) The collimating and magnifying properties of a superconducting field photoelectron spectrometer. J. Phys. E: Sci. Instr. 13, 64-66.

Cazaux J (1984a) How to improve the spatial resolution in X-ray photoelectron spectroscopy and (X-ray-induced) Auger electron spectroscopy. Scanning Electron Microsc. 1984 ; III : 1193-1202.

Cazaux J (1984b) X-ray probe microanalysis and scanning X-ray microscopies. Ultramicroscopy 12, 321-332.

Cazaux J (1985) Prospects in high resolution X-ray photoelectron microscopy. Ultramicroscopy 17, 43-50.

Chaney RL (1987) Recent developments in spatially resolved ESCA. Surface and Interface Analysis 10, 36-47.

Chung MS, Everhart TE (1974) Simple calculation of energy distribution of low-energy secondary electrons emitted from metals under electron bombardment. J. Appl. Phys. 45, (2), 707-709.

Egerton RF (1986) Electron Energy-Loss Spectroscopy in the Electron Microscope. Plenum Press, New York.

Haak HW, Sawatzky GA, Ungier L, Gimzewsky JK, Thomas TD (1984) Core-level electron-electron coincidence spectroscopy. Rev. Sci. Instrum. 55, (5), 696-711.

Jackson JD (1962) Classical Electrodynamics. John Wiley & Sons, Inc., New York, 719.

Kim YK (1972) Angular Distributions of Secondary Electrons in the Dipole Approximation. Phys. Rev. A 6, (2), 666-670.

Kruit P (1986) Electron optics for Auger spectroscopy with high spatial resolution. Proc. XIth Int. Cong. on

Electron Microscopy, Kyoto, Japan, 593-594.

Kruit P, Read FH (1983) Magnetic field parallelizer for 2π electron spectrometer and electron-image magnifier. J. Phys. E: Sci. Instrum. 16, 313-324.

Kruit P, Shuman H (1985) The influence of objective lens aberrations in energy-loss spectroscopy. Ultramicroscopy 17, 263-268.

Kruit P, Venables JA (1988) High-spatial-resolution surface-sensitive electron spectroscopy using a magnetic parallelizer. Ultramicroscopy 25, 183-194.

Reimer L (1983) Scanning Electron Microscopy. Springer-Verlag, Berlin, 144.

Seah MP, Dench WA (1979) Quantitative Electron Spectroscopy of Surfaces: A Standard Data Base for Electron Inelastic Mean Free Paths in Solids. Surface and Interface Analysis 1, No. 1, 2-11.

Tanuma S, Powell CJ, Penn DR (1988) Calculations of Electron Inelastic Mean Free Paths for 31 Materials. Surface and Interface Analysis 11, 577-589.

Turner DW, Plummer IR, Porter HQ (1984) Photoelectron emission: images and spectra. Journal of Microscopy 136, Pt. 2, 259-277.

Ungier L, Thomas TD (1985) Near threshold excitation of KVV Auger spectra in carbon monoxide using electron-electron coincidence spectroscopy. J. Chem. Phys. 82, (7), 3146-3151.

Wiel MJ van der, Brion CE (1972/73) "Photoelectron" spectroscopy by electron impact coincidence measurements of scattered and ejected electrons in CO. J. Electron Spectrosc. 1, 309-318.

## Discussion with Reviewers

R.Reichelt: Does the electrostatic 90° hemispherical deflector significantly effect the primary beam?
Authors: The primary beam will experience a small deflection due to the 90° deflector. At present, to make a scan through the secondary electron energy range we retard all electrostatic elements along the secondary electron path, with respect to the specimen, and do not change the deflection voltage over the 90° deflector. The change in deflection is therefore a second order effect. The shift of the primary beam in the specimen plane can further be reduced if we let the pivot point of the deflection coincide with the intermediate image of the source. Alternatively a Wien filter could be used as beam separator, see Kruit and Venables (1988). A slightly different approach is investigated in Delft, where a design of a crossed electrostatic magnetic field deflector is made, which minimizes the dispersion of the deflector. For a fixed setting of the deflector, a large energy range can be analyzed.

R.Reichelt: To what extend will plural scattering in thin samples create problems using the energy loss of the transmitted electrons to estimate the energy absorbed by the sample atom? What do you consider as a thin sample?
Authors: Plural scattering is indeed a problem as it is in EELS. The effect will be a convolution of the photo electron spectrum with the low-loss EEL spectrum. We are not sure to what extent deconvolution with the low-loss spectrum is applicable for this new technique. The thinner the sample, the better the coincidence technique will work.

R.Reichelt: The pressure in the vicinity of the sample in a EM400 is probably in the range of $10^{-6}$ to $10^{-5}$ Torr. A meaningful surface microanalysis, however, requires a pressure orders of magnitude lower than the one your microscope presently has. Can you make a comment to that?
Authors: With present vacuum conditions contamination of the sample is a known limitation. We are working on the development of a UHV stage-environment and are testing the possibility of sputtering the sample with $Ar^+$ ions during the analysis.

R.Reichelt: What kind of detectors are used to detect the Auger electrons and the inelastically scattered transmitted electrons?
Authors: For the ejected electrons we use a microchannel plate detector (a Galileo circular chevron model 3025.25) and for the energy loss electrons we use a 90° sector magnet with plastic scintillator and photomultiplier (Gatan model 607).

J.Cazaux: In the microprobe approach, the lateral resolution will be independent from that of the parallelizer but it will depend upon the X-ray spot size on the specimen. Taking into account the fact that the thickness of the target has to be increased when the primary beam energy is increased, leading to a deterioration of the lateral resolution, but also an increase of the number of X-ray photons per incident electron, what is your choice for the primary beam energy?
Authors: The choice of primary beam energy, anode thickness and anode material will be strongly dependent on the required spatial resolution and intensity. We cannot add anything to the considerations presented in the reference Cazaux (1984b).

J.Cazaux: From our experiments, Cazaux (1984a/b,1985) and references therein) a 1 μA, 1 μm incident beam on an Al target produces $10^8$, $10^9$ Al Kα photons at 10 keV inside a semi-apex solid angle of around 45°. If you set your target at 1 mm from the specimen, the size of your image will be around 1 mm × 1 mm for a pixel size of 0.1 mm. Is it a problem?
Authors: The selected area photo electron spectroscopy mode to which the reviewer refers is clearly not a high spatial resolution imaging technique, although the selection of a 0.1 × 0.1 mm area can be useful in many photo electron spectroscopy applications. The 'field of view' does not depend on the illuminated area, but rather on the freedom of motion of the specimen. For high resolution imaging with photolectrons in a Scanning Transmission Electron Microscope, the coincidence technique is the most promising option.